

Improvements and verifications for the Spherical Zoeppritz Explorer

Charles P. Ursenbach, Arnim B. Haase and Jonathan E. Downton*

ABSTRACT

A key improvement is given for the Spherical Zoeppritz Explorer. This involves using exponential wavelets, which are employed in the analytical frequency integration, to represent the commonly used Ricker wavelet. In connection with this, the user interface to the applet now accepts the dominant frequency of the wavelet rather than the previous, less intuitive, wavelet parameter, s . We also carry out additional numerical tests to confirm that the methodology of the Spherical Zoeppritz Explorer can yield an extremely accurate approximation to exact results.

INTRODUCTION

In a previous report (Ursenbach and Haase, 2004), a method was presented for efficient calculation of spherical-wave reflection coefficients which employed only very minor approximations. The generalized reflection coefficients associated with spherical waves emanating from a point source can be calculated from the frequency-dependent potential (cf. Aki and Richards, 1980):

$$\phi(\omega) = Ai\omega \exp(-i\omega t) \int_0^\infty R_{PP}(p; \alpha_1, \beta_1, \rho_1, \alpha_2, \beta_2, \rho_2) \frac{p}{\xi} J_0(\omega pr) \exp[i\omega \xi(z+h)] dp. (1)$$

Here $R_{PP}(p; \alpha_1, \beta_1, \rho_1; \alpha_2, \beta_2, \rho_2)$ is the well known plane-wave reflection coefficient given by Zoeppritz, in which p is a ray parameter (the horizontal slowness), α , β , and ρ are P-wave velocity, S-wave velocity, and density, and subscripts 1 and 2 refer to upper and lower media. To complete the description of the equation above, A is a scaling factor, ω is the frequency, t is time, ξ is the vertical P-wave slowness in the upper layer, J_0 is the zeroth-order Bessel function, r is the horizontal receiver coordinate, z is the vertical receiver coordinate, h is the vertical source position, and the horizontal source position is equal to zero.

The displacement is obtained by applying a gradient in the receiver position to the above potential. Weighting by the wavelet and applying an inverse Fourier transform yields the time trace observed at the receiver. AVO information can be extracted from maxima in the trace envelope. The above method was implemented in numerical calculations by Haase (2002, 2003, 2004a) [see also Haase and Ursenbach (2004)]. He has also carried out this procedure for converted waves (Haase, 2004a) and with viscoelasticity (Haase, 2004b).

* Veritas, DGC

The alternative method suggested for efficiency (Ursenbach and Haase, 2004) involves reversing the order of ω and p integrations, and choosing a wavelet of the form

$$f(\omega) \propto \omega^n \exp(-|s\omega|), \quad n = 0, 1, 2, \dots, \quad 0 < s < \infty. \quad (2)$$

which allows the ω -integration to be carried out analytically. This yields a time-dependent seismic trace, but the p -integration must still be carried out for each value of t . As an additional approximation, it is then assumed that t is equal to the arrival time dictated by ray theory. The p -integration is then carried out numerically for this one value of t . The only other approximation is the assumption that displacement occurs precisely along the ray direction. This is not exactly true, particularly in the vicinity of the critical point where the head wave is separating from the reflected wave. We note that this approximation is also made in the more accurate calculations of Haase and Ursenbach (2004). This paper presents numerical tests of both approximations, as well as the effect of approximating a Ricker wavelet by wavelets of the form of equation (2). These tests are carried out in the context of modifications to the Spherical Zoeppritz Explorer, which is based on the above theory. The method of Haase we refer to as a fully numerical method, and the method outlined above we refer to as semi-analytic, as the ω -integration is carried out analytically, and the p -integration numerically.

IMPROVEMENTS TO THE SPHERICAL ZOEPPRITZ EXPLORER

Approximating Ricker wavelets by exponential wavelets

Let us rewrite equation (2) as

$$f_n(\omega) \propto |\omega|^n \exp\left(-\frac{n|\omega|}{\omega_{\max}}\right), \quad \text{where } n = 1, 2, \dots, \text{ and } \omega_{\max} > 0. \quad (3)$$

We have left out the case of $n = 0$, as this allows us to identify ω_{\max} as the dominant frequency. This can be demonstrated straightforwardly:

$$0 = \frac{d}{d\omega} [\omega^n e^{-s\omega}] = \left(\frac{n}{\omega} - s\right) \omega^n e^{-s\omega} \Rightarrow s = \frac{n}{\omega_{\max}}. \quad (4)$$

Equation 3 is reminiscent of the Ricker wavelet,

$$f_{\text{Ricker}}(\omega) = \omega^2 \exp\left[-\left(\omega/\omega_{\max}\right)^2\right], \quad (5)$$

for which ω_{\max} is again the dominant frequency.

Figure 1 shows the $n = 5$ and Ricker wavelets, along with an Ormsby wavelet used earlier (Ursenbach and Haase, 2004). The exponential wavelet clearly appears to be a useful approximation to the Ricker wavelet. Note that for the purposes of this figure we have scaled each of the wavelets by a constant to give

$$f_n(\omega) \propto \left| \frac{e\omega}{\omega_{\max}} \right|^n \exp\left(-\frac{n|\omega|}{\omega_{\max}}\right) \quad (6)$$

and

$$f_{\text{Ricker}}(\omega) \propto e\left(\frac{\omega}{\omega_{\max}}\right)^2 \exp\left[-(\omega/\omega_{\max})^2\right], \quad (7)$$

which normalize the wavelets at their maxima.

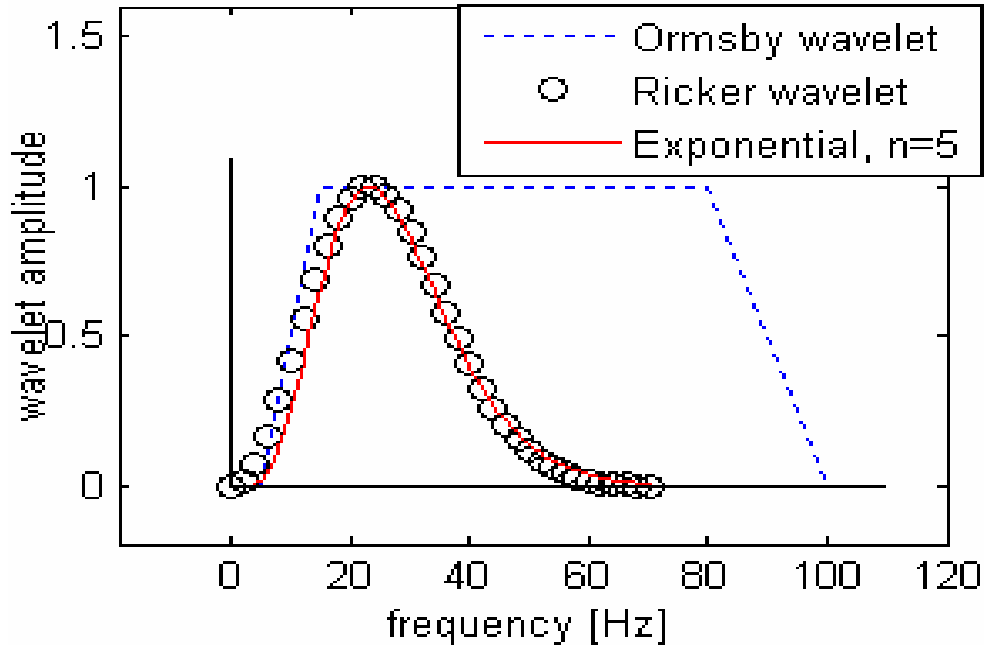


FIG. 1. Comparison of a wavelet of the form of Eq. (3) (solid red line) with a Ricker wavelet (black circles) having the same ν_0 of ~ 23.1 Hz. Also included in the comparison is a 5/15-80/100 Ormsby wavelet (dashed blue line). All three wavelets have similar low-frequency cutoffs.

This figure suggests that f_5 provides an excellent representation of the Ricker wavelet, although for practical purposes in exploration seismology, some other values of n could likely also be used with sufficient accuracy.

In this notation, the quantity $R\omega_{\max}/\alpha_1$ (where R is defined by $R^2 = r^2 + 4h^2$ and is the total pathlength traveled from source to receiver) is a quantity of key importance, as it is a measure of the spherical effects. It is analogous to the quantity kr used to measure spherical effects for monochromatic spherical waves (cf. Krail and Brysk, 1983; Furlong et al., 1994). The quantity $R\omega_{\max}/\alpha_1$ appears frequently in the expressions used to program the Spherical Zoeppritz Explorer.

Modified interface

The updated interface for the Spherical Zoeppritz Explorer is shown in Figures 2 and 3. Figure 2 displays the control panel, where one now enters ν_0 instead of S , and $n = 0$ has been removed as an option, while $n = 5$ has been added. Figure 2 displays the graphical output. The wavelet displays include comparisons of the exponential wavelet employed in the calculation with the Ricker wavelet it approximates. This new version of the explorer should be more intuitive for users, allowing them to think in terms of ν_0 and Ricker wavelets rather than S and exponential wavelets.

ν_0 [Hz]: **Z [m]:**

n=1
 n=2
 n=3
 n=4
 n=5

Dimensionless sphericity parameter: $\alpha_1 / (2Z\nu_0) = 0.086$

incident wave in upper layer

Upper layer density (ρ_1): kg/m³

Upper layer Vp (α_1): m/s

Upper layer Vs (β_1): m/s

incident wave in lower layer

Lower layer density (ρ_2): kg/m³

Lower layer Vp (α_2): m/s

Lower layer Vs (β_2): m/s

Spherical Zoeppritz
 Spherical Aki-Richards

Zoeppritz
 Aki-Richards

Angle limits (integers, 0 to 90):

Magnitude limits:

Phase limits (integers):

[Click here to recalculate graph](#)

Units:
 m/s and kg/m³
 ft/s and g/cm³

FIG. 2. The control panel of the updated Spherical Zoeppritz Explorer. The dominant frequency, ν_0 , is now an input variable, instead of the equivalent but less intuitive S parameter used previously. The parameter n is used to choose which exponential wavelet is employed in the calculation.

CREWES Spherical Zoeppritz Explorer

www.crewes.org

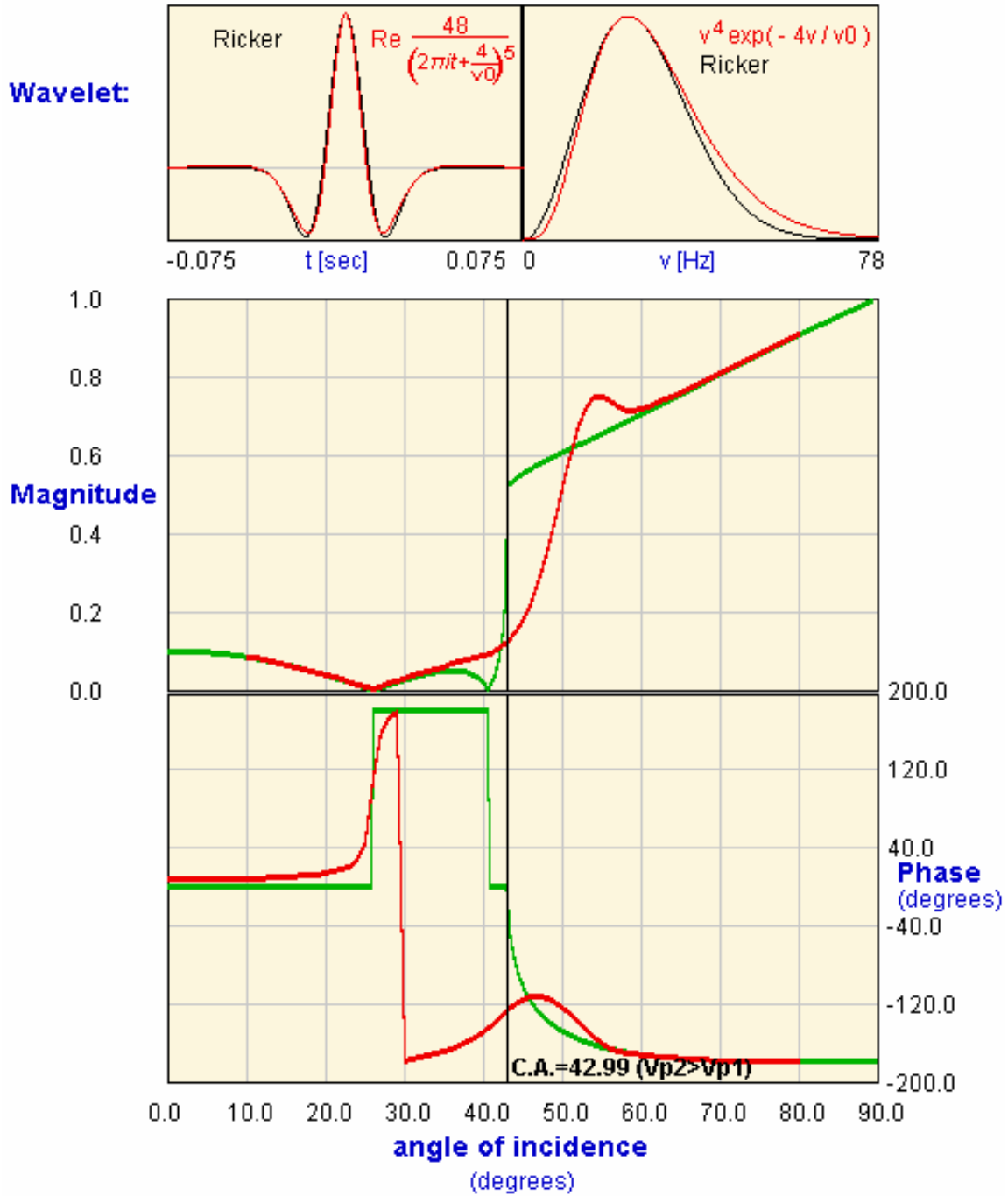


FIG. 3. The graphical output of the updated Spherical Zoeppritz Explorer. The wavelet display shows the exponential wavelet used in the calculation, and compares it with a Ricker wavelet possessing the same dominant frequency, ν_0 .

VERIFICATION OF EXPLORER ACCURACY

We consider three possible sources of error in the Explorer calculations: 1) the approximation of an arbitrary wavelet by an exponential wavelet, 2) the assumption that the arrival time always equals that calculated from ray theory, and 3) the assumption that the wavefront is always normal to the reflected raypath. We will estimate through calculation the error introduced by each of these.

The model we employ for calculations is the same as that employed earlier (Haase, 2004a), namely, an Ormsby wavelet, 5/15-80/100 Hz and the earth model detailed in Table I.

Table I. Earth parameters for a two-layer, Class I AVO model.

	Upper Layer	Lower Layer
V_P (m/s)	2000	2933.33
V_S (m/s)	879.88	1882.29
ρ (kg/m ³)	2400	2000

Exponential wavelet: Ricker and Ormsby wavelets are commonly used in synthetic modeling. It has been previously shown that calculations employing exponential wavelets can provide a rough approximation of calculations with an Ormsby wavelet (Ursenbach and Haase, 2004). This is illustrated in Figure 4.

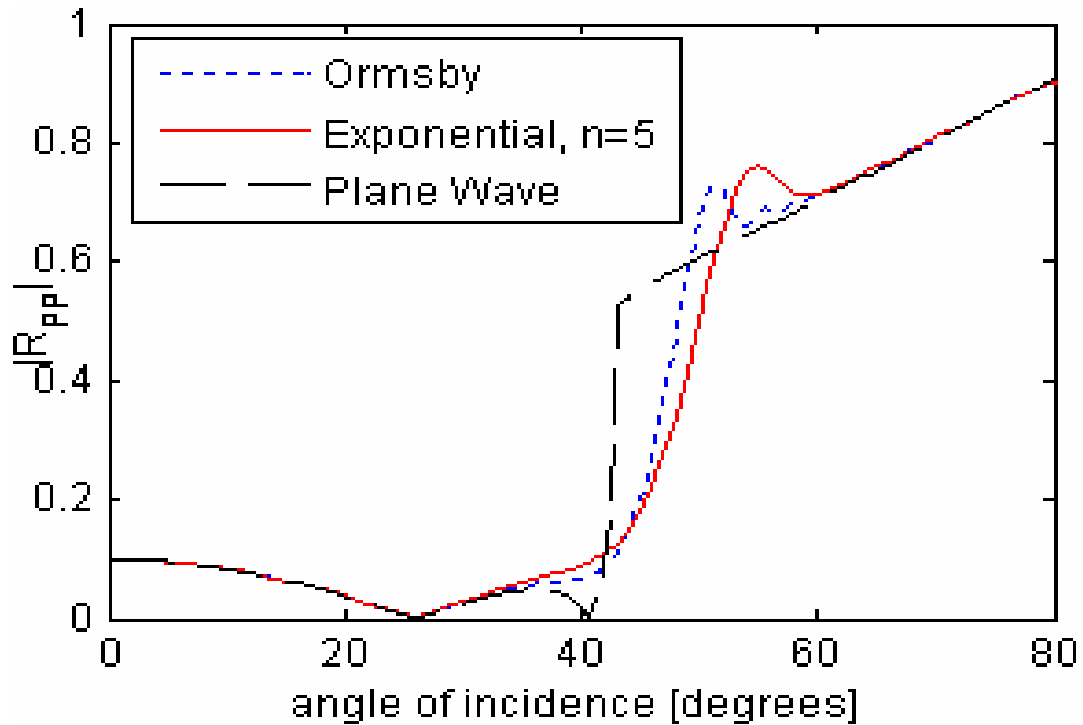


FIG. 4: A comparison of spherical-wave reflection coefficients calculated using an Ormsby wavelet and the exponential wavelet of equation 3. Both have been normalized to allow comparison with the plane-wave result. This figure demonstrates that the exponential wavelet result provides a qualitative approximation to the Ormsby result.

In Figure 5 we show generalized reflections, all calculated by the same fully numerical method, for the Ricker wavelet and for $n = 4, 5$ and 6 exponential wavelets. All are very similar, and the Ricker and $n = 5$ wavelets are indistinguishable on the scale of the figure. Note the scale of the figure, and that results are shown a short distance past the critical angle in a region where differences are the greatest.

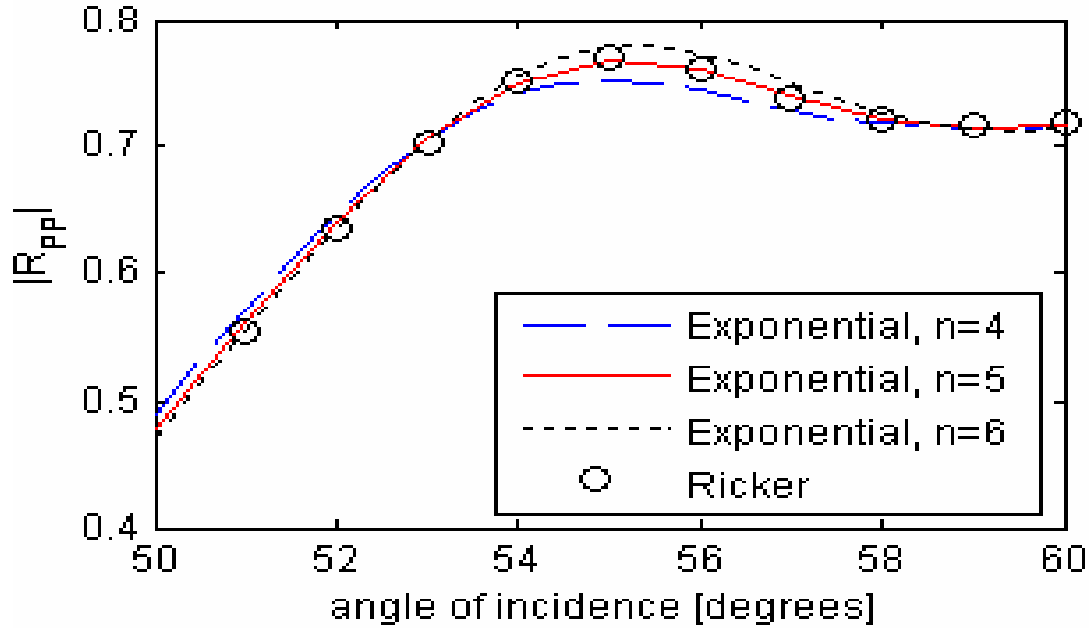


FIG. 5: A comparison of spherical-wave reflection coefficients calculated using a Ricker wavelet and f_4 , f_5 and f_6 of equation 3. All have been normalized for comparison with the plane-wave result. This figure demonstrates that the exponential wavelet result can provide a quantitative approximation to the Ricker result for an appropriate value of n .

Figures 4 and 5 demonstrate that the exponential wavelet required by the Spherical Zoeppritz Explorer methodology can qualitatively represent arbitrary seismic wavelets, and can quantitatively represent certain wavelets, such as the Ricker wavelet.

The arrival time and propagation direction approximations are related to each other, as shown in the Figure 6. In the pre-critical region there is only a simple reflected wave. Far into the critical region there are both reflected and head waves, but they are well-separated at the receiver. Just after the critical point, however, they are both present and interfere with one another. The arrival time and propagation direction of this generalized reflection are not precisely the same as for a simple reflection predicted by ray theory. Thus the errors from these approximations are greatest for angles slightly greater than the critical angle.

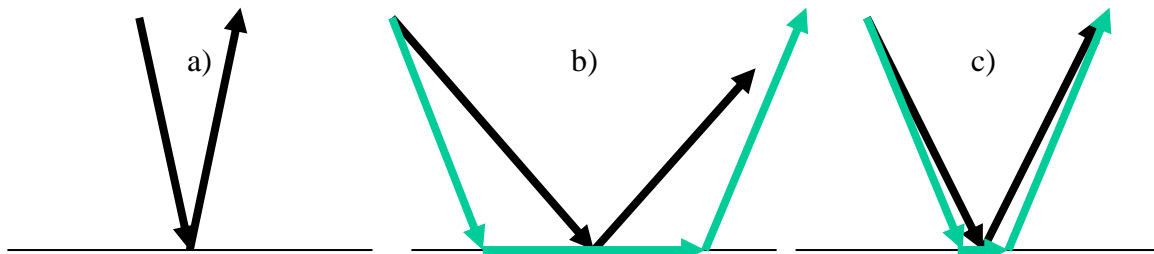


FIG. 6: A diagram representing a) pre-critical reflecting wave, b) reflected and head waves well past the critical point, and c) reflected and head waves immediately past the critical point.

Arrival time: If we employ the same exponential wavelet in both numerical and semi-analytical calculations, the arrival time will be the only theoretical source of error, as the calculations of Haase locate the arrival time from the full time trace. This approximation is thus tested by comparing calculations of these two methods for identical systems. Such a comparison is shown in Figure 7 (which was also shown in Ursenbach and Haase (2004), and is included here for completeness). Figure 7a shows both curves together, nearly indistinguishable, and Figure 7b shows the difference, with the critical point located by the green vertical line. The largest differences, which are still small in absolute terms, are immediately after the critical point, as reflected and head waves are separating from one another.

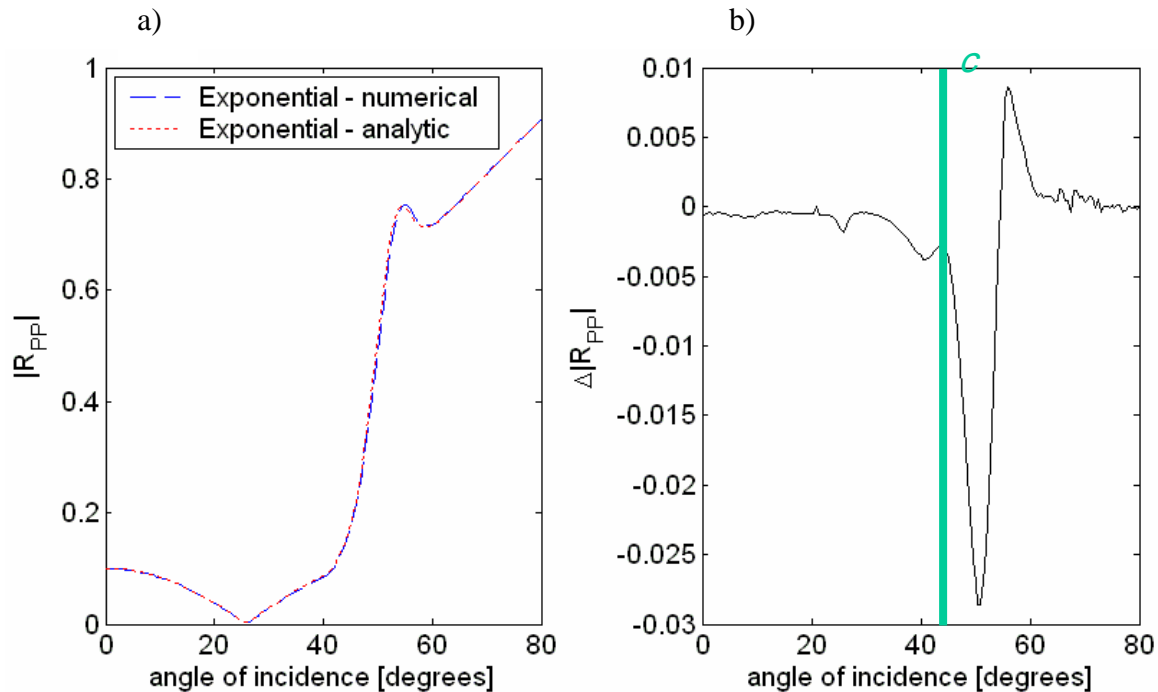


FIG. 7: a) The spherical reflection coefficient for an exponential wavelet calculated by both fully numerical and semi-analytical methods. b) The difference between curves in a), which constitutes a measure of the error introduced by assuming the ray-theory prediction of arrival time. The error is greatest just past the critical angle.

Propagation direction: Both the numerical and the semi-analytical method presented in this paper employ this approximation, so the following approach was devised to estimate its effect. P-waves have displacements parallel to the direction of propagation, so any deviation would manifest itself as a displacement normal to it. A modification was made to the fully numerical calculation to allow calculation of displacements perpendicular to the ray direction, and these are displayed as the black dotted line in Figure 8. This figure again shows that the perpendicular component becomes largest in the region immediately following the critical point, and that, even at its maximum, this component is still considerably smaller than the parallel component. For comparison the errors of Figure 7b (red solid) and the $n = 5$ error implied by Figure 5 (blue dashed) have also been included. It is clear that these approximations will introduce no substantive error into the calculation.

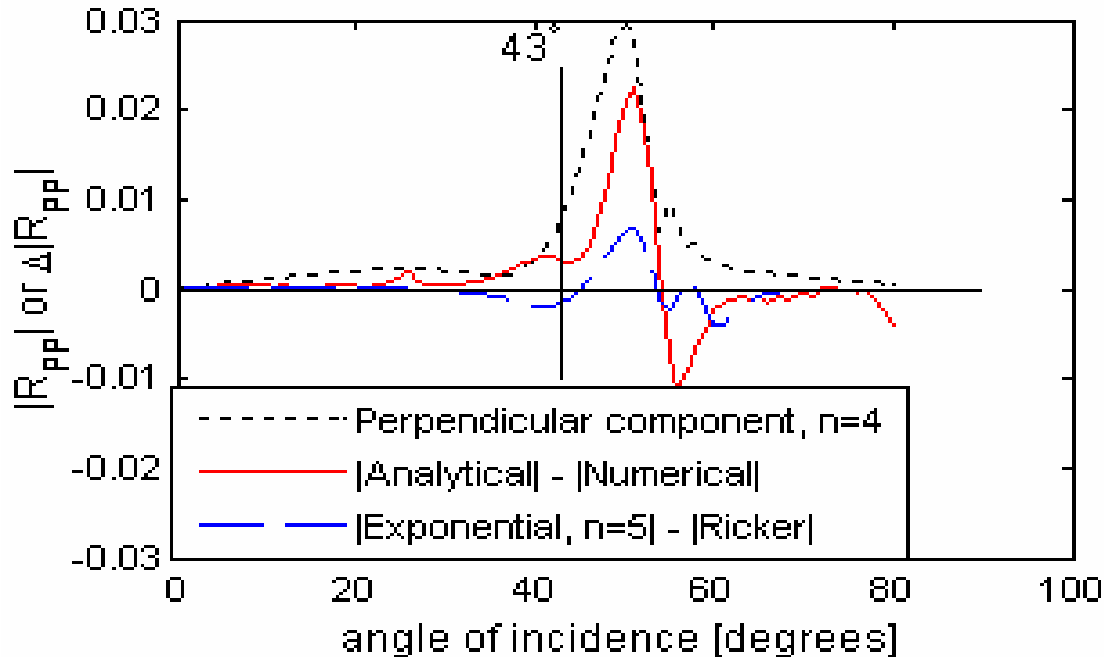


FIG. 8: A representation of all of the errors present in the Spherical Zoeppritz Explorer methodology. The black dotted and red solid lines represent the error from assuming that the direction of propagation and arrival times are given by ray theory. The blue dashed line is the error from assuming that the exponential $n = 5$ wavelet is equivalent to the Ricker wavelet. All three errors are greatest just past the critical point, and all are negligibly small in absolute terms.

CONCLUSIONS

The Spherical Zoeppritz Explorer introduced previously (Ursenbach and Haase, 2004) has been markedly improved. The parameter s employed previously, which measured the rate of exponential decay of the wavelet, has been replaced by ω_0 (or ν_0), the dominant frequency of the wavelet. This contains equivalent information, but is much more intuitive and accessible to most exploration geophysicists. Comparison with Ricker wavelets is now made explicit in the Explorer display, which are also defined by their dominant frequency.

All of the approximations inherent in the Explorer methodology have been identified, and the magnitude of their associated errors has been estimated by appropriate calculations. It is shown that all errors are negligibly small if one is assuming a Ricker wavelet. For other arbitrary wavelets, the error will be dominated by the wavelet effect, but the results will still be qualitatively correct.

REFERENCES

- Aki, K. and Richards, P. G., 1980, Quantitative Seismology: Theory and Methods: W.H. Freeman, 1980.
 Furlong, J.R., Westbury, C.F., and Phillips, E.A., 1994, A method for predicting the reflection and refraction of spherical waves across a planar interface: *J. Appl. Phys.*, **76**, 25-32.
 Haase, A.B., 2002, Plane waves, spherical waves and angle-dependent P-wave reflectivity in elastic VTI-models, SEG Expanded Abstracts.
 Haase, A.B., 2003, Approximation Errors in AVO-Analysis and Inversion, CSEG Expanded Abstracts.
 Haase, A.B., 2004a, Spherical Wave AVO Modelling of Converted Waves in Elastic Isotropic Media, CSEG Expanded Abstracts. [See also Haase, A.B. and Ursenbach, C.P., 2004, Spherical wave AVO-modelling in elastic

- isotropic media, CREWES Research Report (this volume). This paper contains similar calculations to the CSEG abstract, but with the same normalization method as the present study.]
- Haase, A.B., 2004b, Spherical Wave AVO Modeling of Converted Waves in Isotropic Media, SEG Expanded Abstracts.
- Haase, A.B. and Ursenbach, C., 2004, Spherical-wave AVO modelling in elastic isotropic media, CREWES Research Report, Vol. 16.
- Krail, P.M. and Brysk, J., 1983, Reflection of spherical seismic waves in elastic layered media: *Geophys.*, **48**, 655-664.
- Ursenbach, C. and Haase, A.B., 2004, An efficient method for calculating spherical-wave reflection coefficients, CREWES Research Report, **16**.